CrossMark

ORIGINAL PAPER

Thin films of V_2O_5/MoO_3 and their applications in electrochromism

C. M. Cholant[1] · T. M. Westphal[1] · R. D. C. Balboni[1] · E. A. Moura[2] · A. Gündel[3] ·
W. H. Flores[3] · A. Pawlicka[4] · C. O Avellaneda[1]

Abstract Pure and doped vanadium pentoxide (V_2O_5, V_2O_5/MoO_3) thin films were prepared by sol-gel method and dip coating technique. Furthermore, they were characterized by chronocoulometry, cyclic voltammetry (CV), UV-Vis, atomic force microscopy (AFM), X-ray diffraction (XRD), and perfilometry. The best results were obtained with V_2O_5/MoO_3 5 mol% film, which showed highest ion storage capacity of ~92 mC cm^{-2} when compared to other films. Moreover, this film showed optical modulation of 40% at 633 nm after coloration and bleaching for 60 s. XRD patterns revealed that the film has orthorhombic crystalline structure; AFM and perfilometry confirmed roughness and thickness of 4.38 and 554 nm, respectively.

Keywords Sol-gel process · Thin film · V_2O_5/MoO_3

Introduction

Electrochemical and optical properties of metal oxide films are directly related to their physical and chemical characteristics such as stoichiometry, presence of impurities and defects,

nucleation process and crystals coalescence, morphology, degree of crystallinity, and the crystal structure [1]. On the other hand, performance of an electrochromic system can be measured by electrochromic efficiency, contrast or transmittance variation (ΔT), response time for a material to change color, and its electrochemical stability, which ideally should not wear out when subjected to several cycles of color change.

Vanadium pentoxide (V_2O_5) thin film is a very interesting material because the insertion of lithium ions (Li$^+$) in its structure leads to an alteration of transparency. This occurs during the oxidation and reduction processes (redox) when film undergoes color changes of yellow-green-blue. As reported in many scientific papers, V_2O_5 has excellent electrochromic properties [2] and high storage capacity of Li$^+$ ions, which is related to its layered orthorhombic structure [3] and makes the material promising for various applications. On the other hand, literature also shows that films of V_2O_5 have low ionic conductivity, low cyclic stability, and low reversibility during the insertions and extraction cycles, limiting their practical use [4]. These unfavorable properties are due to an increase of the electrical resistance produced by ions that are trapped in V_2O_5 crystalline structure, resulting in slight structural distortions. However, another studies suggest that adding other transition metal oxides as for example molybdenum oxide, which change color from transparent to blue [5], titanium oxide (transparent to dark blue) [6], niobium oxide (transparent to blue) [7], and hydrated iridium oxide (transparent to dark blue) [8] in vanadia matrix minimize its poor electrical properties. As an example, electrochromic performance of mixed V_2O_5/MoO_3 15 mol% thin films synthesized by pulsed spray pyrolysis technique showed an increased charge density of 35 C cm^{-2} and good stability [9].

In this context and aiming to find a best dopant quantity, this article presents a systematic study of V_2O_5 thin films doped with different concentrations of MoO_3 and compare it

✉ C. O Avellaneda
cesaravellaneda@gmail.com

1   Centro de Desenvolvimento Tecnológico, Universidade Federal de Pelotas, Rua Félix da Cunha, 806, Centro, Pelotas, RS 96010-00, Brazil

2   Instituto de Física e Matemática - IFM, Universidade Federal de Pelotas, Capão do Leão, RS, Brazil

3   Universidade Federal de Pampa, Rua Travessa 45, n° 1650, Bagé, RS 96413-170, Brazil

4   IQSC-USP, Av. Trabalhador Sãocarlense 400, São Carlos, SP 13566-590, Brazil

Springer

to pure V_2O_5. The evaluation of the samples was performed through chronocoulometry, which pointed to the best sample in terms of charge capacity storage. This sample was then subjected to cyclic voltammetry (CV), UV-visible (UV-Vis) spectroscopy, as well as morphological and structural measures such as atomic force microscopy (AFM), X-ray diffraction (XRD), and perfilometry.

Experimental

Preparation of the sols and thin films

The sol of V_2O_5 was prepared from a mixture of vanadium (V) oxytriisopropoxide (Sigma-Aldrich), isopropyl alcohol (Synth) as solvent, and glacial acetic acid (Synth) as catalyzer [10]. V_2O_5/MoO_3 sol was obtained by adding 2 to 15 mol% of molybdenum isopropoxide (V) (Alfa Aesar) to the V_2O_5 sol.

Fluor tin oxide (FTO; Pilkington) plates were cleaned by immersion in acetone (Synth), isopropyl alcohol, and distilled water under ultrasonic irradiation for 15 min each. The films were deposited on FTO substrates (1 cm × 3 cm) by dip coating technique at 10, 15, and 20 cm min^{-1} rate. The layers were deposited one over other in such a way that after deposition each layer was densified at 350 °C for 10 min. Finally, three layer films were heat treated at 350 °C for 30 min. The mass of samples was 0.7 ± 0.1 mg. The samples with best visual morphology were subjected to analyses.

Characterization of thin films

The electrochemical measurements were performed with a potentiostat/galvanostat (Autolab PGSTAT 302N) and using a conventional electrochemical cell of three electrodes. A platinum foil with 1 cm^2 was a counter-electrode, and a silver wire was a reference electrode. The electrolyte was a 0.1 mol L^{-1} lithium perchlorate (LiClO$_4$) (Vetec) dissolved in propylene carbonate (PC; Sigma-Aldrich). Potential range of −0.85 to +0.85 V was applied. The electrochromic properties of thin films were studied by UV-Vis (Agilent Technologies Cary 100) in the range from 400 to 800 nm. Spectra were collected for unpolarized films, polarized (colored), and depolarized (discolored).

The structural characterizations were done by XRD (Rigaku Ultma IV diffractometer) by using CuK_{α} radiation and Bragg-Brentano geometry.

Morphological studies were performed with perfilometer (Veeco Dektak D-150) and AFM (Agilent Technologies 5500) on 1 μm × 1 μm sample's area.

Results and discussion

Systematic study of a charge capacity of the doped and undoped films

Figure 1 presents the results of cathodic (Q_c) and anodic (Q_a) charge densities of pure V_2O_5 [10] and V_2O_5/MoO_3 films as a function of MoO_3 content, which were obtained by chronocoulometry measurements at −0.85 and +0.85 V applied during 60 s each. Analyzing these results, one can observe that addition of MoO_3 from 0 to 5 mol% into the matrix of V_2O_5 caused an increase of the charge density from 102 to maximum of 132 mC cm^{-2} mg^{-1}, respectively. For higher MoO_3 content, a successive decrease of the charge density is observed, and for 15 mol% of MoO_3 in V_2O_5 matrix the charge is only 88 mC cm^{-2} mg^{-1}. Moreover, all the films revealed very good electrochemical reversibility rate of cathodic (Q_c) to anodic (Q_a) charge equal to 1.

Cyclic voltammetry measurements

Figure 2 presents second cycle of cyclic voltammetries of V_2O_5 and V_2O_5/MoO_3 with 5 mol% that are composed by two cathodic (−0.2 and −0.5 V) and two anodic (0.3 and 0.6 V) peaks, which are related to colored and bleached processes, respectively. The first cathodic peak (j_{pc1}) describes a potential when a small fraction of the V^{5+} ions are reduced to V^{4+}, and the remaining reduction process occurs at the potential of the second peak (j_{pc2}). The same happens with anodic process, and peaks j_{pa1} and j_{pa2} correspond to reversible process occurred at j_{pc1} and j_{pc2}, respectively [10]. The voltammogram presented in our paper is very similar to V_2O_5 voltammograms already published by other authors. All of them observed two cathodic and two anodic peaks, which were explained as two different phases of $Li_xV_2O_5$ [11, 12], and which was already shown by Dickens and Reynolds [13].
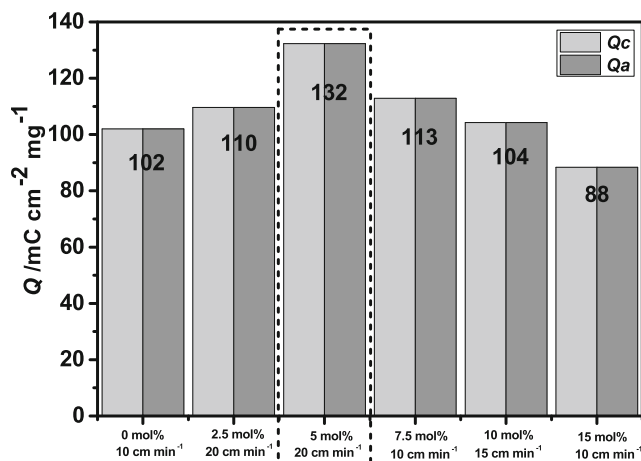

Fig. 1 Charge density values as a function of MoO_3 content in V_2O_5 matrix obtained by applying −0.85 and +0.85 V for 60 s each
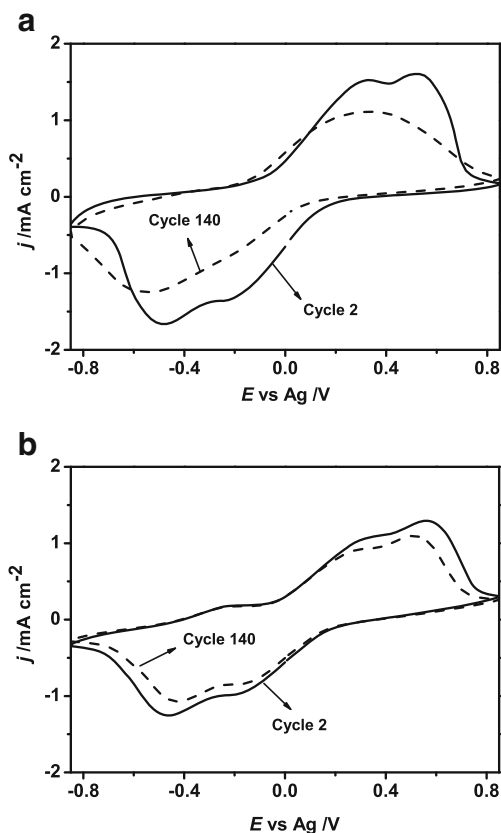
Fig. 2 Voltammograms of 2nd and 140th cycles at scan rate of 20 mV s^{-1}. **a** V_2O_5 film and **b** V_2O_5/MoO_3 5 mol% film

Additionally, to evaluate the electrochemical stability, which is important for application in electrochromic or any other devices, the analyzed material was subjected to 140 cycles of coloring and bleaching (Fig. 2a). The results of these measurements show that the V_2O_5 film loses its electrochemical stability because anodic and cathodic current peak intensities decrease and change the shape for one large peak each (Fig. 2a). This can be due to some ions and electrons that remain trapped in the V_2O_5 matrix [10]. On the other hand, voltammogram of V_2O_5/MoO_3 (Fig. 2b) reveals almost the same shape and intensity as for the second cycle, confirming its better electrochemical stability and corroborating other reports [5]. Moreover, a small decrease of the peak intensities (Fig. 2b) was due to the preferential reduction from Mo^{3+} to Mo^{2+} that prevents the reorganization of V_2O_5 structure [14].

UV-Vis spectroscopy measurement

Figure 3 shows the transmittance curves of V_2O_5 and V_2O_5/MoO_3 5 mol% films in order to obtain performance of the films in colored and bleached states. The measurements were performed in wavelength range of 400 to 800 nm after cathodic potential of −0.85 V application for 60 s. At 633 nm, a transmittance of V_2O_5 film decreases from 81 to 40% (Fig. 3a), and at the same time, a transmittance of V_2O_5/MoO_3 5 mol% decreases from 73 to 33% (Fig. 3b).

Fig. 3 In situ transmittance results (**a**, **b**) and data replotted for direct and indirect allowed transitions (**c**, **d**) of V_2O_5 (**a**, **c**) and V_2O_5/MoO_3 5 mol% film (**b**, **d**) as deposited (*solid lines*), colored at −0.85 V (*dashed lines*), and discolored +0.85 V (*dotted lines*). *Insets* show the films in each state
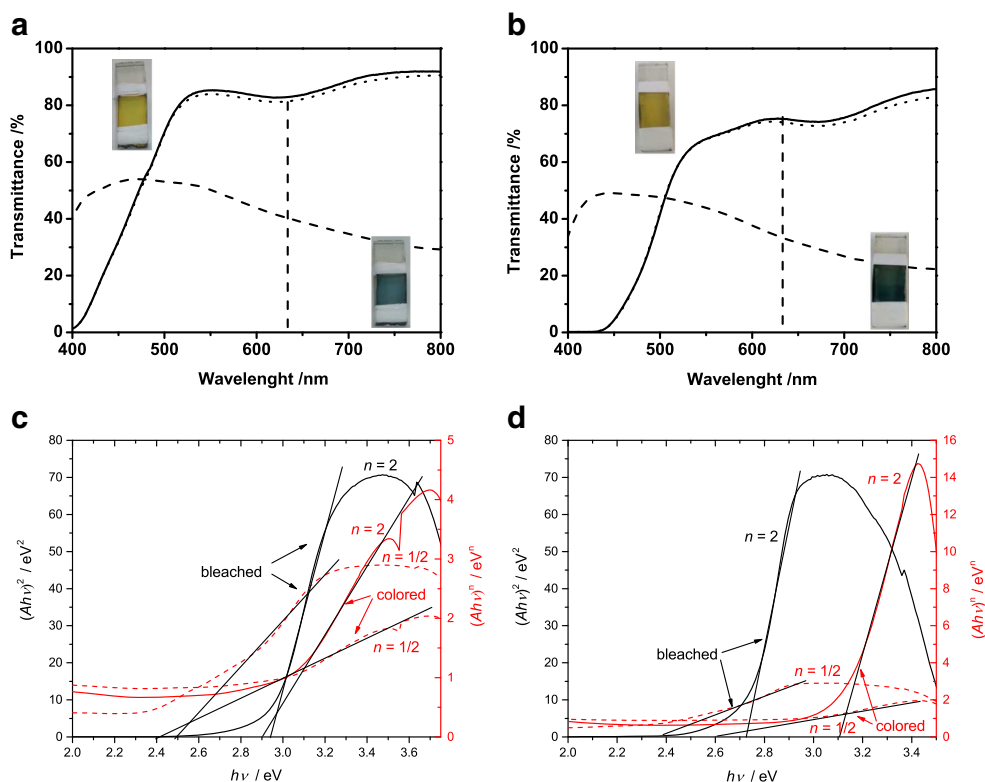
Consequently, the difference of transmittance (ΔT) between color and bleached states is 41 and 40% for pure and doped vanadia film, respectively. Therefore, vanadia-based thin films have an excellent electrochromic performance, and because they transmit less than 40% of light in their color state, they are capable to obtain a control up to 80% of the daylight [15]. Besides that, a comparison between those two films reveals that V_2O_5/MoO_3 5 mol% film has lower transmittance values, in the whole 400 to 800 nm range, than V_2O_5, which makes it better at blocking the visible light.

Films before and after the electrochemical insertion/extraction present a gradual color change from yellow (V_2O_5 film) [11] to blue (V_2O_5/MoO_3 films), and it is observed that a presence of dopant leads to a darker coloration.

The coloration efficiency, η, is defined as the ratio of optical density at a particular wavelength to the charge inserted in the coloration process for unit electrode area [16] and is given in Eq. 1.

$$\eta(\lambda) = \frac{\Delta OD(\lambda)}{q/A} = \frac{\ln\left(T_b / T_c\right)}{Q_i}, \tag{1}$$

where T_b and T_c are the transmittances of the sample in the bleached and colored state, respectively. Q_i is the amount of charge intercalated into the sample to cause change in optical density (ΔOD), and (q/A) is the charge intercalated per unit electrode area.

The estimated values of optical density for the samples of V_2O_5 and V_2O_5/MoO_3 5 mol% were 0.19 and 0.21, respectively. Sample V_2O_5/MoO_3 had higher transmittance modulation, and this improved its optical density. Consequently, this sample had coloration efficiency of 0.82, which is similar to 0.73 of V_2O_5. Faughnan and Crandall [17] reported that in composite oxides is believed to take place $V^{4+} \rightarrow Mo^{2+}$ transition in addition to the intervalence charge transfer between adjacent ions ($Mo^{2+} \rightarrow Mo^{3+}$, $V^{4+} \rightarrow V^{5+}$). According to this preferential model of mixed-metal oxides, electrochromic efficiency can be enhanced through additional electron intervalence transfer between two kinds of metal sites. Hence, it was established that V_2O_5/MoO_3 exhibited better electrochromic properties, which is consistent with other reported results [10].

Transmission values of V_2O_5 and V_2O_5/MoO_3 (Fig. 3a, b) were then used to obtain the values of optical band gap (E_g) by using Tauc [18] and Davis and Mott model [19] $(\alpha h\nu)^n = B(h\nu - E_g)$, where $h\nu$ is the photoenergy, α is the absorption coefficient ($\alpha = A/d$; A is absorbance and d is a thickness of the film), B is the constant related to the transition probability of material, and n indicates either 2 or ½ for direct and indirect allowed transition, respectively [20–22]. As the thickness of the films was the same in colored and bleached states and B is a constant, this equation can be simplified to

$(Ah\nu)^n \propto (h\nu - E_g)$. Figure 3c shows a plot of $(Ah\nu)^n$ versus $h\nu$ for $n = 2$ and ½ for V_2O_5 colored and bleached films. The energy band gaps obtained by extrapolating linear fits to $y = 0$ were 2.90 and 2.94 eV for $n = 2$ and 2.41 and 2.50 eV for $n = ½$ for colored and bleached states of the films, respectively. The values of indirect allowed transitions are comparable to 2.44 eV obtained for polycrystalline V_2O_5 thin films [23]. However, in this study, better linear fittings were obtained with $n = 2$ when compared to $n = ½$, which indicates direct allowed transitions. The results of optical band gap determination for films of V_2O_5/MoO_3 are shown in Fig. 3d. Again, better linear fittings were obtained with $n = 2$ and resulted in E_g of 3.11 and 2.73 eV for $n = 2$ and 2.60 and 2.37 eV for $n = ½$ for colored and bleached states of these films. These values are in between E_g values of 3.35 and 2.44 eV for polycrystalline MoO_3 and V_2O_5 thin films [23], confirming a mix structure of the molybdenum-doped vanadium pentoxide thin films.

Kinetic measurement

Kinetic measurements, shown in Figs. 4 and 5, were performed in situ in order to analyze an electrochromic response time of the films. The films were polarized and depolarized under cathodic and anodic potential application for 60 s, and the time of coloration and discoloration was measured in a wavelength of 633 nm. For example, lithium ion insertion in the film matrix throughout a cathodic potential application turned the films blue colored (Fig. 3, inset) because their charge density increased and redox reactions occurred and, consequently, their transmittances decreased (Fig. 3).

Figure 4 shows the results of kinetic measurements of V_2O_5 film, where one can see that in 60 s the film reached 70 mC cm^{-2} and a transmittance of 35%; V_2O_5/MoO_3 5 mol% film (Fig. 5a) reached 91 mC cm^{-2} and transmittance of 32% under the same experimental condition. Moreover, already after 13 and 18 s of charge insertion into V_2O_5 and V_2O_5/MoO_3 5 mol% films, respectively, a transmittance decreased from 57 to 34% for undoped film (Fig. 5c), 60 to 32% for doped film, and the charge density values were of 47 and 59, respectively. The extraction of charges occurred in 15 (Fig. 4c) and 20 s (Fig. 5c) and reached the values of 70 and 87 mC cm^{-2} for undoped (Fig. 4b) and doped (Fig. 5b) films, respectively. In a general way, a kinetic of polarization of electrochromic films occurs more slowly than the depolarization; however, in the present case, almost the same times were observed for insertion and extraction of charges.

X-ray diffraction

Figure 6 shows the XRD patterns for the V_2O_5 and V_2O_5/MoO_3 5 mol% films that reveal well-defined diffraction peaks attributed to an orthorhombic polycrystalline structure with

Fig. 4 Kinetic measurement for V$_2$O$_5$ film **a** chronocoulometry, **b** chronoamperometry, **c** transmittance, and **d** optical density in function of the applied potential at λ = 633 nm
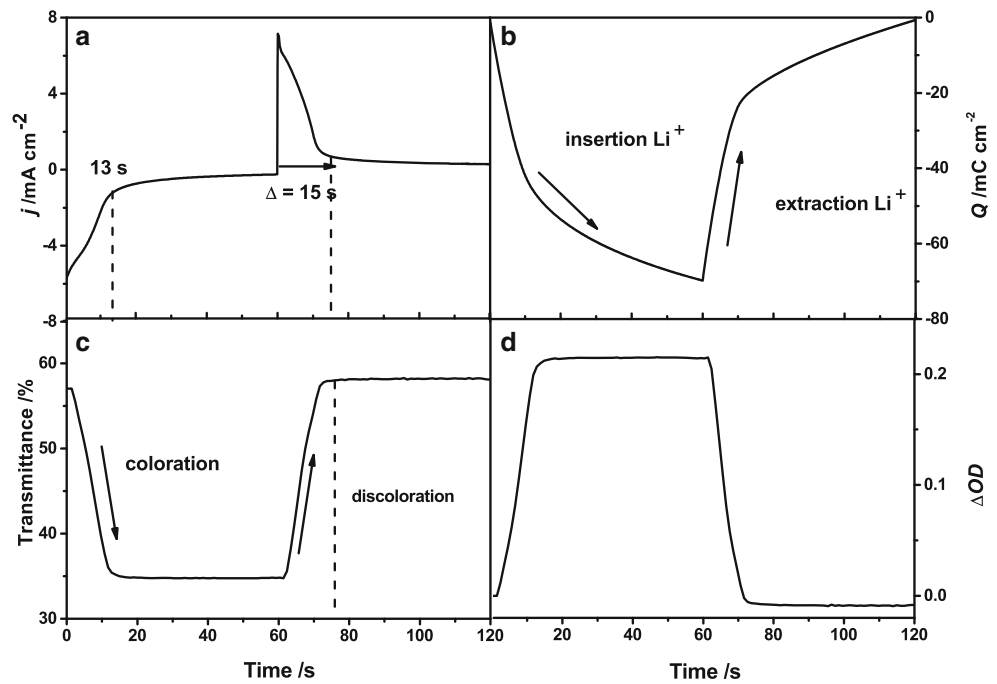
lattice parameters of a = 11.516, b = 3.565, and c = 4.372 Å, according to the default [PDF 41-1426] for V$_2$O$_5$. The FTO substrate peaks are indicated by points in Fig. 6.

In film of crystalline V$_2$O$_5$, the diffractogram presents a narrow peak in the region of 2θ = 20.2° that is related to the crystalline plan (001). The type of the morphology can be obtained by comparing the diffractogram peaks, where the larger peaks are characteristic of materials with low degree of crystallinity, while the narrow ones are characteristic of crystalline materials or materials with high degree of crystallinity. The widths at half

height of these peaks can give information about the crystallite size that is large for low width at half height value [24].

Analyzing the diffractograms in Fig. 6, one can see narrow peaks characteristics of crystalline materials among which the most intense is situated at 2θ = 20.3°. This peak is related to the crystalline plan (001), which is typical of a stacking lamellar structure [25]. Moreover, it is also observed that intensity of the peak related to this plan (001) increases with the presence of dopant, and there is a small shift to lower 2θ resulting in an interplanar distance of 4.3689 Å for V$_2$O$_5$ film and of

Fig. 5 Kinetic measurements for V$_2$O$_5$/MoO$_3$ 5 mol% film. Chronocoulometry (**a**), chronoamperometry (**b**), transmittance (**c**), and optical density (**d**) in function of applied potential and measured at λ = 633 nm
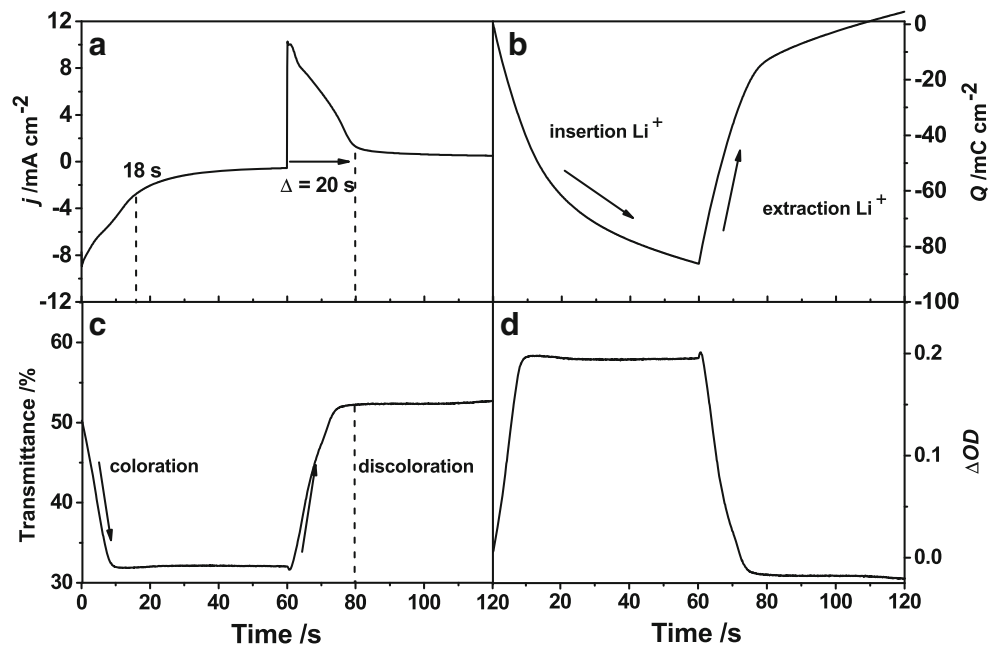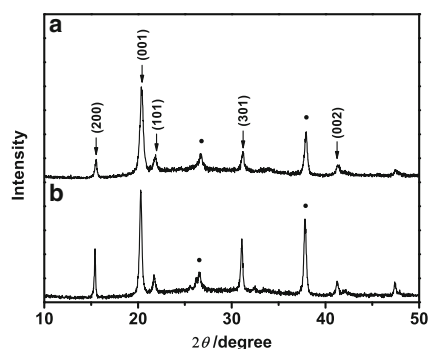
Fig. 6 XRD patterns of **a** V_2O_5 and **b** V_2O_5/MoO_3 5 mol%. FTO substrate peaks are identified with dots

4.3710 Å for V_2O_5/MoO_3 5 mol%, indicating an enlargement of the interplanar distances of the film after doping.

The undoped and doped vanadia films' crystallite sizes were measured based on the enlargement of the diffraction peak corresponding to (001) plane using the Debye-Scherrer [26] Eq. 2.

$$D = 0.95\lambda \Big/ \beta \; \cos\theta, \qquad (2)$$

where D is the crystallite size, λ is the wavelength of the incident radiation, $\lambda = 1.54$ Å of CuK_α, θ is the Bragg angle, and β is an instrumental correction ($\beta = \left(\beta_f^2 - \beta_b^2\right)^{1/2}$, where β_f^2 belongs to the film and β_b^2 to the reference film). Equation 2 calculi resulted in the values of crystallite size of 21.5 and 25.9 nm for V_2O_5 and V_2O_5/MoO_3 5 mol% film, respectively.

Li and Kudo [27] considered two kinds of intercalating sites in mixed Mo/V amorphous films, and they called them homogeneous and separated clusters. The homogenous clusters were composed by polyanions of vanadium and molybdenum linked together, and the others were separated from each other. In our case, it is seen similar diffractograms and voltammograms of pure and molybdenum-doped vanadium pentoxide. However, as the diffractograms are similar and addition of dopant only promoted an increase of interplanar distance and crystallite size, so this increase of crystallite size can be due to the formation of only homogenous clusters.

Atomic force microscopy (AFM) microanalysis

Figure 7 shows typical AFM 3D images of FTO substrate, V_2O_5, and V_2O_5/MoO_3 5 mol% films of 1×1 μm^2 area. Surface of FTO (Fig. 7a) presents nanostructured well-distributed grains with elliptical shape and RMS = 18.38 nm. This structure allows a good interaction between substrate and film. V_2O_5 layer (Fig. 7b) has small rugosity with RMS = 5.13 nm and thickness of 265 nm. Addition of MoO_3 5 mol% to V_2O_5 matrix promotes a formation of film with still smaller nanostructured grain on its surface, which has RMS = 4.38 nm and thickness of 554 nm (Fig. 7c).
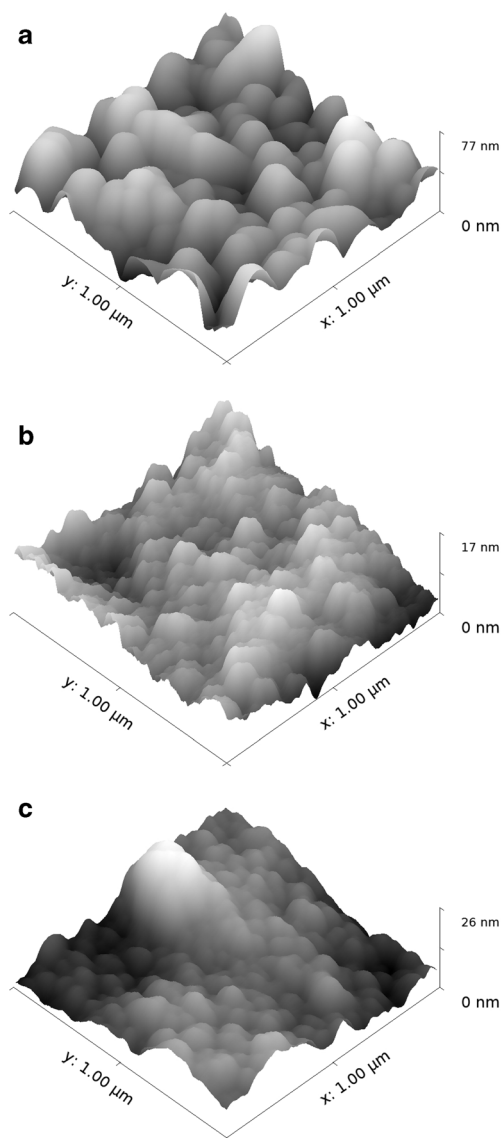

Fig. 7 AFM image of **a** FTO substrate, **b** V_2O_5 thin film, and **c** V_2O_5/MoO_3 5 mol% thin film

Conclusions

In this article, thin films of V_2O_5/MoO_3 were studied, characterized, and compared to pure V_2O_5 films. All the films were prepared by the sol-gel process and deposited by dip coating technique, proving to be effective for such films synthesis. Moreover, sols for V_2O_5/MoO_3 deposition were stable, homogeneous, and easy to prepare, and the obtained physical-chemical results revealed to be better that for pure V_2O_5 films. The CV measurements of the V_2O_5/MoO_3 5 mol% thin film demonstrated that the insertion/extraction process is reversible, presenting a charge density with maximum value of 92 mC cm^{-2} in 60 s of −0.85 V application for three-layer film deposited at a speed of 20 cm min^{-1}. The transmittance values at 633 nm revealed changes of 41 and 40%; the charge insertion times were of 13 and 18 s and extraction of 15 and 20 s for

pure and doped vanadia film, respectively. The XRD allowed the identification of the orthorhombic polycrystalline phase and the crystallite size of 21.51 and 25.90 nm for V_2O_5 and V_2O_5/MoO_3 5 mol% film, respectively. The AFM measurements showed that the films' surfaces have smooth formations and elliptical grains. V_2O_5 film's RMS was of 5.13 nm and thickness of 265 nm, and for V_2O_5/MoO_3 5 mol% films RMS value was of 4.38 nm and thickness of 554 nm.

In summary, the obtained results were satisfactory, showing that the addition of molybdenia dopant provided improvements in the physical and chemical properties of V_2O_5 film. This behavior indicates that the methodology and the procedures used here were adequate, and these films are promising in the implementation as counter-electrode in electrochromic devices.

References

1. Rosario A, Pereira E (2002) Optimisation of the electrochromic properties of Nb2O5 thin films produced by sol–gel route using factorial design. Sol Energ Mat Sol Cells 71:41–50

2. Bahgat A, Ibrahim F, El-Desoky M (2005) Electrical and optical properties of highly oriented nanocrystalline vanadium pentoxide. Thin Solid Films 489:68–73

3. Suresh R, Giribabu K, Manigandan R, Kumar SP, Munusamy S, Muthamizh S, Narayanan V (2014) Characterization and dopamine sensing property of V2O5@ polyailine nanohybrid. Synth Met 196: 151–157

4. Kim H-K, Seong T-Y, Yoon YS (2003) Structural study of amorphous vanadium oxide films for thin film microbattery. J Vac Sci Technol B 21:754–759

5. Scarminio J, Lourenco A, Gorenstein A (1997) Electrochromism and photochromism in amorphous molybdenum oxide films. Thin Solid Films 302:66–70

6. Harizanov O, Harizanova A (2000) Development and investigation of sol–gel solutions for the formation of TiO2 coatings. Sol Energ Mat Sol Cells 63:185–195

7. Schmitt M, Heusing S, Aegerter MA, Pawlicka A, Avellaneda C (1998) Electrochromic properties of Nb2O5 sol-gel coatings. Sol Energ Mat Sol Cells 54:9–17

8. Nishio K, Watanabe Y, Tsuchiya T (1999) Preparation and properties of electrochromic iridium oxide thin film by sol-gel process. Thin Solid Films 350:96–100

9. Patil C, Jadhav P, Tarwal N, Deshmukh H, Karanjkar M, Patil P (2011) Electrochromic performance of mixed V2O5–MoO3 thin films synthesized by pulsed spray pyrolysis technique. Mat Chem Phys 126:711–716

10. Westphal TM (2015) Thin films of V2O5 doped with Nb2O5. Master thesis, Federal University of Pelotas, Brazil

11. Monk PMS, Mortimer RJ, Rosseinsky DR (2007) Electrochromism and electrochromic devices. Cambridge University Press, New York

12. Cogan SF, Nguyen NM, Perrotti SJ, Rauh RD (1989) Proc. 1988 International Congress on Optical Science and Engineering

13. Dickens PG, Reynolds GJ (1981) Proceedings of the International Conference on Fast Ionic Transport in Solids Transport and equilibrium properties of some oxide insertion compounds. Solid State Ionics 5:331–334

14. Lin Y-S, Lai J-Y, Tsai T-H, Chuang P-Y, Chen Y-C (2011) Effects of oxygen addition on electrochromic properties in low temperature plasma-enhanced chemical vapor deposition-synthesized MoO x C y thin films for flexible electrochromic devices. Thin Solid Films 519:3875–3882

15. Wittkopf H, Proc. Glass Processing Days Conference, Tampere, Finland, September 13–15, 1997

16. Inamdar AI, Kim Y, Jang B, Im H, Jung W, Kim D-Y, Kim H (2012) Effects of oxygen stoichiometry on electrochromic properties in amorphous tungsten oxide films. Thin Solid Films 520:5367–5371

17. Faughnan BW, Crandall RS (1977) Optical-properties of mixed-oxide WO3-MoO3 electrochromic films. Appl Phys Lett 31:834–836

18. Tauc J (1974) Optical properties of amorphous semiconductors. In: Tauc J (ed) Amorphous and liquid semiconductors. Plenum Publishing Company Ltd, New York, pp 159–200

19. Davis E, Mott N (1970) Conduction in non-crystalline systems V. Conductivity, optical absorption and photoconductivity in amorphous semiconductors. Phil Mag 22:0903–0922

20. Khan GA, Hogarth CA (1991) Optical absorption spectra of evaporated V2O5 and co-evaporated V2O5/B2O3 thin films. J Mater Sci 26:412–416

21. Bouzidi A, Benramdane N, Nakrela A, Mathieu C, Khelifa B, Desfeux R, Da Costa A (2002) First synthesis of vanadium oxide thin films by spray pyrolysis technique. Mater Sci Eng B 95:141–147

22. Al-Sehemi AG, Al-Shihri AS, Kalam A, Du G, Ahmad T (2014) Microwave synthesis, optical properties and surface area studies of NiO nanoparticles. J Mol Struct 1058:56–61

23. Boudaoud L, Benramdane N, Desfeux R, Khelifa B, Mathieu C (2006) Structural and optical properties of MoO3 and V2O5 thin films prepared by spray pyrolysis. Catal Today 113:230–234

24. Decker F, Donsanti F, Salvi AM, Ibris N, Castle JE, Martin F, Alamarguy D, Vuk AS, Orel B, Lourenco A (2008) Li+ distribution into V2O5 films resulting from electrochemical intercalation reactions. J Braz Chem Soc 19:667–671

25. Winter M, Brodd RJ (2004) What are batteries, fuel cells, and supercapacitors? Chem Rev 104:4245–4270

26. West AR (2007) Solid state chemistry and its applications. Wiley India Pvt, Limited, India

27. Li Y-M, Kudo T (1995) Properties of mixed-oxide MoO 3/V 2 O 5 electrochromic films coated from peroxo-polymolybdovanadate solutions. Sol Energ Mat Sol Cells 39:179–190